University of *Ljubljana*
Faculty of *Mathematics and Physics*

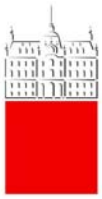

Department of Physics

Seminar

Torsional Instability of Elastic Rods

Manca Podvratnik
Advisor: prof. dr. Rudolf Podgornik

May 19, 2011

Abstract

Twisting a piece of string at some point causes the string to become buckled. Further twisting that piece of string will eventually cause it to coil around itself, forming a helix-like structure. This is something that all of us have observed at some point in our lives. However, finding an analytical description of these everyday phenomena is the subject of this paper. Starting with Kirchhoff's elastic rod theory we are able to predict the point at which the piece of string will buckle. We are also able to describe the post-buckled states with an approximate analytical description. Finally, an application of this theory is represented in a DNA supercoiling experiment.

Contents

1 Introduction

The study of elastic rods is a field of research that is interesting in itself because it gives rise to beautiful and complex mathematical structures. Understanding elastic rods is however also important for applications in different fields of research.

In engineering, they are used to study the behavior of submarine cables. Marine cables under low tension and torsion on the sea floor undergo a buckling process during which torsional energy is converted to flexural energy. The cable becomes highly contorted with loops and tangles [1]. This can permanently damage the cable. Also, the study of multi-filament structures such as yarns is interesting for the textile industry.

In biology, rod models are used to describe the supercoiling of DNA molecules. A supercoiled DNA molecule resembles the shape of the buckled marine cable. Because the length of DNA can be thousands of times that of a cell, packaging this genetic material into the cell or nucleus would be difficult if not for supercoiling. Supercoiling of DNA reduces the space and allows for a lot more DNA to be packaged.

In physics, the study of twisted rods is useful in several applications, for example in hydrodynamics for describing of the motion of vortex tubes, or in the study of polymers.

Kirchhoff's theory of elastic rods is the basis for any further study of torsional instability. We know from experience that twisting the rod causes it to buckle. The stability condition for twisted rods under tension is derived through Love's eigenvalue analysis of the solutions to Kirchhoff's equations [2]. Further twisting causes the rod to first come into self-contact and then gradually coil around itself. Coyne [3] recently obtained the instability point at which the rod comes into self-contact. An analytical description of the post-buckled states is also described in [4] [5] [6].

2 Kirchhoff's theory of elastic rods

Kirchhoff's theory describes bending and twisting of thin elastic rods. In Kirchhoff's theory a rod is a three-dimensional body with two dimensions that are considerably smaller then the third. The rod is represented with a space curve $\mathbf{r} = \mathbf{r}(l)$, where the parameter l is the arc length of the curve. The unit tangent vector is

$$\mathbf{t} = \frac{d\mathbf{r}}{dl} = \dot{\mathbf{r}}(l). \tag{1}$$

The term $\dot{\mathbf{r}}(l)$ in a sense represents the velocity of propagation along the space curve (instead of propagation in time).

Suppose the origin of a frame of three orthogonal axes ξ, η, ζ to move along the central line of a rod with unit velocity. Let the ζ axis have the direction of the tangent vector $\mathbf{t}$ and the ξ, η axes have the direction of the principal axes of the cross section so that ξ, η, ζ form a right handed system (figure 1). At this point we assume that the cross section remains undistorted and normal to the center-line of the

rod. We will consider only the case when the cross section is a simply connected region and the geometric center lies within the cross section [7]. This excludes open or closed thin-walled cross sections.

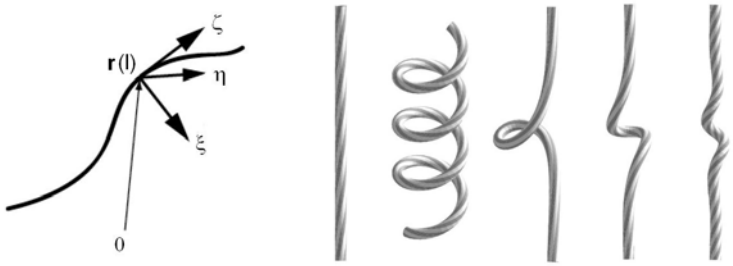

Figure 1: The $\xi\eta\zeta$ frame moves along the length of the rod with unit velocity (left) [8]. The figure also shows selected solutions to Euler-Kirchhoff's equations that are important in the study of instability of elastic rods (right) [8].

Let us consider the angular velocity $\mathbf{\Omega}$ with which this frame rotates along the rod.

$$\begin{pmatrix} \dot{\mathbf{e}}_\xi(l) \\ \dot{\mathbf{e}}_\eta(l) \\ \dot{\mathbf{e}}_\zeta(l) \end{pmatrix} = \mathbf{\Omega}(l) \times \begin{pmatrix} \mathbf{e}_\xi(l) \\ \mathbf{e}_\eta(l) \\ \mathbf{e}_\zeta(l) \end{pmatrix}. \tag{2}$$

We may express the angular velocity with components directed along the instantaneous positions of the principal axes ξ, η, ζ. We denote these components by $\mathbf{\Omega}(l) = (\kappa_1(l), \kappa_2(l), \tau(l))$, where κ_1 and κ_2 are components of curvature of the central line along local ξ and η axes, and τ is the torsion of the rod.

We now wish to obtain equations of equilibrium of a thin rod. We will only consider the case where a thin rod is held bent and twisted by forces and couples applied at it's ends alone[2]. Starting with the condition that an infinitesimal section of the rod is in equilibrium we arrive at the condition

$$\dot{\mathbf{M}} = \mathbf{F} \times \mathbf{t}, \tag{3}$$

where $\mathbf{M}$ is the internal torque and $\mathbf{F}$ is the external force applied at the rod's ends. At this point we need to incorporate some basic physical principles into our exact mathematical theory. The torque of a rod in linear theory of elasticity can be written as

$$\mathbf{M} = EI\mathbf{t} \times \dot{\mathbf{t}} + C\tau\mathbf{t}, \tag{4}$$

where I is the area of the cross section (this expression is only valid for symmetrical cross sections), C is the torsional rigidity of the rod, and E is Young's modulus. The first summand in equation 4 represents the torque that keeps the rod curved and is normal to the plane spanned by $\mathbf{t}$ and the normal $\mathbf{n}$. The second summand represents the torque that keeps the rod twisted and has the direction of $\mathbf{t}$. Our theory from this point onward is no longer exact, but rather an approximation of linear elasticity.

Expressing the internal torque and terminal force in the $\xi\eta\zeta$ frame gives a set of equations of equilibrium of a thin rod that has a symmetrical simply connected cross section

$$\begin{aligned} EI\dot{\kappa_1} + (C - EI)\kappa_2\tau &= \mathbf{F} \cdot \mathbf{e}_\eta \\ EI\dot{\kappa_2} + (EI - C)\kappa_1\tau &= -\mathbf{F} \cdot \mathbf{e}_\xi \\ C\dot{\tau} &= 0. \end{aligned} \tag{5}$$

These equations are sometimes called Euler-Kirchhoff's equations. Euler-Kirchhoff's equations have many solutions in theory, but not all solutions can be observed in reality. Figure 1 shows some solutions that have a physical importance in the study of torsional instability. A trivial solution is a rod that is internally twisted, but remains straight. A continuous helix as well as a localized helix-like deformation also represent possible solutions.

2.1 Kirchhoff's kinetic analogue

Equations of equilibrium of a thin rod, held bent and twisted by forces and couples applied at it's ends alone, can be identified with the equations of motion of a heavy rigid body about a fixed point [2]. A rod

with a symmetric cross section can therefore be identified with the motion of a symmetric top. Equations of motion for a symmetric top are the same as equations 5, where EI and C are replaced by the principal moments of inertia J and $J_{\zeta\zeta}$, and κ_1, κ_2, τ are replaced by components of angular velocity.

In the case of the bent and twisted rod, the role of angular velocity is replaced by torsion and local curvatures (elements of $\mathbf{\Omega}$). Another difference is that there is no time parameter in Kirchhoff's theory of rods, the role of time is played by position along the central line of the rod l. Understanding the parallel between the motion of a rigid body and the deformation of a rod will help us visualize the deformations better. A spinning top can be compared to a twisted rod whereas precession of a spinning top can be compared to a twisted rod bent into helical form [8].

2.2 Euler angle parametrization

According to Euler's rotation theorem, any rotation in space may be described using three angles. This is equivalent to saying that any rotation matrix can be decomposed as a product of three elemental rotation matrices (rotations about a single axis). The three angles ϕ, θ, ψ are called Euler angles and give three separate elemental rotation matrices. There are several ways of choosing Euler angles – we are interested in the so-called zyz convention. As the name suggests, the first elemental rotation will be the rotation of the reference xyz frame through an angle ϕ about the z axis. This rotates the first and second axis in the xy plane. In particular, the second axis now points in the direction of y'. Next we rotate the frame through an angle θ about the new y' axis. This moves the third axis z'' in any assigned orientation in space. Finally, we rotate the frame about z'' through whatever angle ψ is needed to bring the axes into their final assigned directions [9]. The final rotation matrix R is a product of the following three elemental rotation matrices

$$R(\phi, \theta, \psi) = R_z(\psi) R_y(\theta) R_z(\phi), \tag{6}$$

where indices z and y tell us about which axis the frame rotates.

Just as with motion of a rigid body, it is convenient to parameterize equilibrium equations of a rod using Euler angles. We will represent the orientation of the $\xi\eta\zeta$ frame in terms of a reference xyz frame with the help of Euler angles. The rotation matrix R is directly connected to the antisymmetric angular velocity matrix Ω ($\Omega = \dot{R}R^T$). We find the elements of Ω to be

$$\begin{aligned} \Omega_1 = \kappa_1 &= \dot{\theta}\sin\psi - \dot{\phi}\sin\theta\cos\psi \\ \Omega_2 = \kappa_2 &= \dot{\theta}\cos\psi + \dot{\phi}\sin\theta\sin\psi \\ \Omega_3 = \tau &= \dot{\psi} + \dot{\phi}\cos\theta. \end{aligned} \tag{7}$$

The force applied at the rod's ends expressed with Euler angles is $\mathbf{F}_{\xi\eta\zeta} = R(\phi, \theta, \psi)\mathbf{F}_{xyz}$. Finally we can write equilibrium equations (5) with Euler angle parametrization

$$\begin{aligned} C\dot{\phi}\dot{\psi} + (C - EI)\dot{\phi}^2\cos\theta &= F \\ \dot{\psi} + \dot{\phi}\cos\theta &= const. \end{aligned} \tag{8}$$

There are only two equations because the first two of euations 7 yield the same result.

Figure 2 shows Euler angles and their derivatives. It is evident, that Ω_3 is the sum of $\dot{\psi}$ and the projection of $\dot{\phi}$ onto the ζ axis. With the help of figure 2, we could have in fact guessed all three elements of Ω.

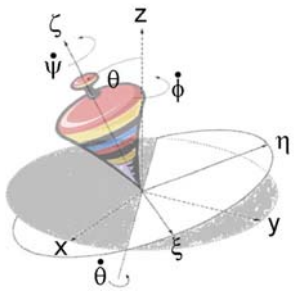

Figure 2: Euler angles and their derivatives [10]. For precession of a spinning top or a rod bent into a helix, the θ angle is constant.

2.3 Rod bent into helical form

Rod bent into a helical form is an important solution of Euler-Kirchhoff's equations. It is also important for another reason. The post-buckled state of a rod, where a rod begins to coil around itself forming a plectonemic region, can be described as two inter-winding helices. Let us consider precession of a spinning top or a rod bent into a helix, where the angle θ is constant. We then find that $\dot{\psi}$ and $\dot{\phi}$ are constants of 'motion' and this gives us our specific solution. The procedure is pretty straight-forward. Putting $\dot{\theta} = 0$ and introducing a new angle $\alpha = \pi/2 - \theta$ gives us

$$\begin{aligned} \kappa &= -\dot{\phi}\cos\alpha \\ \tau &= \dot{\psi} + \dot{\phi}\sin\alpha. \end{aligned} \tag{9}$$

The curvature of the center-line of the rod is constant. Torsion is composed of two parts – internal twist $\dot{\psi}$ and tortuosity $1/\Sigma = \dot{\phi}\sin\alpha$ [2]. Unlike internal twist, tortuosity is a property of the shape of the center-line.

A helix is a curve of constant curvature and tortuosity. It is uniquely defined by two geometrical quantities. These quantities may either be curvature κ and tortuosity $1/\Sigma$ or pitch and radius of the cylinder on which the helix lies. Let R be the radius of the cylinder. We already know that α is the angle that the tangent makes with the xy plane at any point on the helix. The parametrization of a helix is then

$$\mathbf{r}(\phi) = \left(R\cos\phi, R\sin\phi, \frac{h}{2\pi}\phi\right), \quad \phi = \frac{l\cos\alpha}{R}, \tag{10}$$

where h is a constant giving the vertical separation of the helix's loops or the pitch and l is the free parameter that equals the length of the curve. On the other hand, the curvature and tortuosity of a helix are given by

$$\begin{aligned} \kappa &= \tfrac{R}{R^2+(h/2\pi)^2} = \tfrac{\cos^2\alpha}{R} \\ \tfrac{1}{\Sigma} &= \tfrac{h/2\pi}{R^2+(h/2\pi)^2} = \tfrac{\sin\alpha\cos\alpha}{R}. \end{aligned} \tag{11}$$

The geometric connection $h = 2\pi R\sin\alpha/\cos\alpha$ was used to obtain the expressions on the right. We may express all important physical quantities in terms of α and R

$$\begin{aligned} \kappa &= \tfrac{\cos^2\alpha}{R} \\ \dot{\phi} &= \tfrac{\cos\alpha}{R} \\ \dot{\psi} &= \tau - \tfrac{\cos\alpha\sin\alpha}{R}. \end{aligned} \tag{12}$$

It is important to understand that in our case, τ is determined with a boundary condition and is not a variable. Let us not forget that a trivial solution to the Euler-Kirchhoff's equations ($\mathbf{r}(l) = (0,0,l)$) will always exist. It represents a rod that experiences uniform internal twist and remains straight along the z axis.

3 Stability of twisted rods subjected to tensile force

Finding a solution to Euler-Kirchhoff's equations of equilibrium is not a sufficient description of elastic rods. We need to study the stability properties of solutions to the Euler-Kirchhoff's equations. Such a study is fundamental because only stable solutions can be realized experimentally. Unstable solutions, although existing in theory, can never be observed.

Consider initially a straight elastic rod of length L, loaded at it's ends by a constant tensile force F (figure 3 a). We then start to twist the rod, slowly increasing τ. It is clear that at first the rod will remain straight. But if we continue to further twist the rod, this trivial solution will become unstable at a critical point (F_c, τ_c) [4]. At this point the total energy of deformation reduces by decreasing the torsional deformation and, according to Love [2], bending the rod into a helix. The helix at this point is energetically more convenient then the straight rod. This continuous helix is not necessarily always observed. Oftentimes this metastable state is replaced by an energetically more convenient localized helix (figure 3 c).

If we further increase τ, the rod will first come into self-contact (figure 3 e) as described by Coyne [3], and eventually writhe as shown in figure 3 f. It is a physical phenomena that we have all observed at some point in our lives, but probably never thought twice about it.

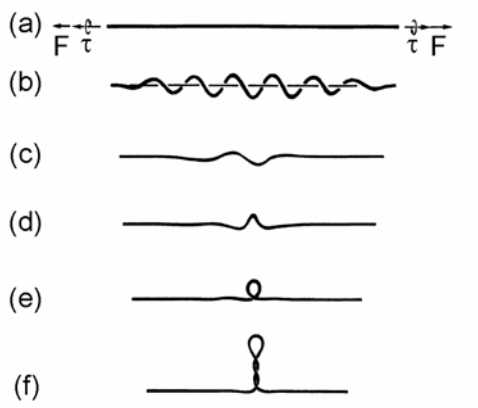

Figure 3: Elastic rod loaded at it's ends by a constant tensile force F and twisted with the torsion coefficient τ [4]. The constant force allows the ends of the rod to approach one another with increasing τ. The rod initially remains straight (a). When increasing τ, we can sometimes observe the formation of a continuous helix (b). On the other hand, the localized helix as described by Coyne in [5] can always be observed (c and d). The rod then comes into self contact (e) and finally coils around itself forming a plectonemic region (e).

3.1 Linear eigenvalue analysis of Love

We can obtain the critical point (F_c, τ_c) of the helix formation as predicted by Love [2] through eigenvalue analysis. Let us first have another look at equation of equilibrium for a thin elastic rod in the xyz reference frame. We need to assume that the central-line of the rod is very nearly straight. The tangent vector therefore reduces to approximately $\mathbf{t} = (\dot{x}, \dot{y}, 1)$. Equation of equilibrium with the condition that $\dot{\tau} = 0$ translate to a set of equations

$$\begin{array}{c} -EI\dddot{y} + C\tau\ddot{x} + F\dot{y} = 0 \\ EI\dddot{x} + C\tau\ddot{y} - F\dot{x} = 0 \\ \dot{x}\ddot{y} - \dot{y}\ddot{x} = 0. \end{array} \tag{13}$$

The third equation is nonlinear and seems to eliminate any nontrivial solution. This is why we will only take into consideration the first two equations. We search for a more general solution of the approximated Kirchoff's equations in the form

$$\begin{array}{l} x(l) = A\cos(q_1 l + \varepsilon_1) + B\cos(g_2 l + \varepsilon_2) \\ y(l) = A\sin(q_1 l + \varepsilon_1) + B\sin(g_2 l + \varepsilon_2). \end{array} \tag{14}$$

Both expressions share the same coefficients A and B. In the case of the spinning top this approximate solution represents nutation. Taking this ansatz into equation 13 we find that

$$q_{1,2} = \frac{C\tau}{2EI} \pm \sqrt{\frac{(C\tau)^2}{(2EI)^2} - \frac{F}{EI}}. \tag{15}$$

The terminal force F is positive for tension and negative for thrust. Taking into consideration the loading conditions $x(0) = y(0) = x(L) = y(L) = 0$ we obtain two sets of equations

$$\begin{pmatrix} \cos\varepsilon_1 & \cos\varepsilon_2 \\ \sin\varepsilon_1 & \sin\varepsilon_2 \end{pmatrix} \begin{pmatrix} A \\ B \end{pmatrix} = 0 \qquad \begin{pmatrix} \cos(q_1 L + \varepsilon_1) & \cos(q_2 L + \varepsilon_2) \\ \sin(q_1 L + \varepsilon_1) & \sin(q_2 L + \varepsilon_2) \end{pmatrix} \begin{pmatrix} A \\ B \end{pmatrix} = 0. \tag{16}$$

In order to obtain nontrivial solutions the determinant of both systems must be 0. The first nontrivial solution of the new equations gives the condition of stability $|q_1 - q_2| = 2\pi$. Using equation 15 we find that a rod subjected to tension F and torsion τ is stable if

$$\frac{F}{EI} > \frac{(C\tau)^2}{(2EI)^2} - \frac{\pi^2}{L^2}. \tag{17}$$

The more we twist our rod (increase τ) the greater the tensile force F has to be in order to keep the rod straight. We see that for zero force the critical torsion equals $\tau_{c0} = 2\pi\sqrt{EI}/CL$ and is very small for

long rods. A long twisted rod almost instantly buckles if there is no tensile force to keep it straight. For very long rods the right-most term of equation 17 may be neglected to obtain a simplified condition

$$F_c = \frac{(C\tau_c)^2}{4EI}. \tag{18}$$

At this critical point the rod will buckle into a three-dimensional helix with axial wavelength $\Lambda_c = 2\pi/q = 2\pi\sqrt{EI/F_c}$ (this can be easily obtained from (15) and (17)). An interesting consequence of this simplified criticality condition is that the complete number of turns made by the end moment per incipient helical wave is

$$\frac{\Lambda_c}{2\pi/\tau_c} = \frac{2EI}{C} = 2(1+\nu). \tag{19}$$

We used the fact that the torsional rigidity equals $C = JG = EI/(1+\nu)$, where G is the torsional stiffness ($G = E/2(1+\nu)$), J is the principal moment of inertia (for a circular cross-section $J = 2I$) and ν is the Poisson ratio. This is a delightfully general result, depending only on the Poisson ratio and independent of the applied tension [4]. For soft rubber the Poisson ratio is approximately 1/2. This tells us that a rubber rod will form a helix with 3 turns per wave at the critical point.

3.2 White's theorem

White's Theorem states [8] that the linking number Lk of a curve is the sum of it's twist number Tw and it's writhe number Wr (figure 4)

$$Lk = Tw + Wr, \tag{20}$$

and that Lk is constant for a closed curve no matter what shape it takes. The linking number of a rod measures the number of twists that have gone into it in order to create it [5]. It is usually associated with closed rods, but can be applied to an open rod as well.

Here Tw represents the internal twist $\dot{\psi}$. The twisting number for a rod can be obtained with the formula

$$Tw = \frac{1}{2\pi}\int \dot{\psi} dl. \tag{21}$$

On the other hand, the writhe number Wr is a property of the shape of the curve. We shall not investigate the writhe number in mathematical detail. Suffice it to say that Wr is the numberer of positive crossings minus the number of negative crossings that a curve makes with a surface. Figure 4 should help us visualize the writhe number better. The ribbon on the right has the twist number equal to 2.5 and the writhe number equal to zero ($Lk = Tw + Wr = 2.5$). The ribbon on the left has large Wr and very small Tw.

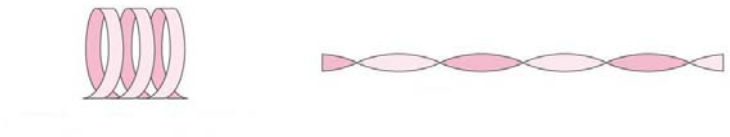

Figure 4: The writhe number of the ribbon on the left is large and the twist number is very small. On the other hand, the ribbon on the right has $Wr = 0$ and $Tw = 2.5$ [11].

A good way to visualize White's theorem is to imagine a telephone cord. Stretching the cord to it's maximum will result in increasing Tw so that Wr becomes 0. No matter whether the cord is stretched or not, the linking number Lk does not change.

At first it might seem that White's theorem is just a restatement of the expression for torsion τ (equations 7, 9 and 12). As mentioned, Love's torsion is a sum of two parts – internal twist and tortuosity ($\tau = \dot{\psi} + \cos\alpha \sin\alpha/R$). Internal twist is directly proportional to the twist number. The tortuosity, however, is not to be confused with the writhe number.

The condition that τ is constant holds throughout the length of the rod. As soon as we change the boundary conditions (for example stretch the rod), τ will change it's value but still remain constant along the length of the rod. However, stretching will not cause the linking number to change.

3.3 Coyne's localized solution

James Coyne [3] took a different approach to describing torsional instabilities when studying cable mechanics in undersea systems. His approach assumes that the solutions are localized, restricted to the middle of the cable as depicted in figure 3 c - e. Another important variable apart from torsion τ and tension F is introduced – cable ends displacement B. Suppose initially a straight cable with twist τ_0. Letting the two ends approach one another changes the torsion and tension. A loop begins to form. Coyne's analysis gives this missing relation between torsion, tension and end displacement up to the point when the cable comes into self-contact.

We need to first upgrade our understanding of Kirchoff's theory. Let us try to find the 'constants of motion', or quantities that remain constant throughout the length of the rod, since no actual motion is present. The first constant is easy enough to guess – energy or rather energy per unit length of the cable

$$h = \frac{1}{2}EI\kappa^2 + \frac{1}{2}C\tau^2 + F\cos\theta = \frac{1}{2}EI\left(\dot{\theta}^2 + \dot{\phi}^2\sin^2\theta\right) + \frac{1}{2}C\left(\dot{\psi} + \dot{\phi}\cos\theta\right)^2 + F\cos\theta. \tag{22}$$

The first two summands represent flexural and torsional energies. It is a bit more difficult to justify the last summand. In the kinetic analogue it represents the potential energy of the spinning top in a gravitational field where $F = mg$. For an elastic rod, it represents the potential energy because of the force applied at the rod's ends. Euler-Lagrange equations for the cyclic coordinates ψ and ϕ give another two 'constants of motion'

$$p_\psi = C(\dot{\psi} + \dot{\phi}\cos\theta) = C\tau, \tag{23}$$

$$p_\phi = EI\dot{\phi}\sin^2\theta + C(\dot{\psi} + \dot{\phi}\cos\theta)\cos\theta. \tag{24}$$

Equation 23 is no surprise. It states that the torsion (which is the sum of internal twist and tortuosity) is the same at every cross section along the rod. Equation 24 expresses the condition that, at every cross section, the moment about a line passing through the cable cross section parallel to the z axis is constant.

The cable is assumed to be long compared with the loop that forms. It is essentially straight at it's ends. We may assume that θ and $\dot{\theta}$ vanish at cable ends. The constants at cable ends therefore equal $h = F + 1/2C\tau^2$ and $p_\phi = p_\psi = C\tau$. Taking these expressions into equations 22 and 23 gives a set of equation for $\dot{\theta}$ and $\dot{\phi}$

$$\frac{1}{2}EI\left(\dot{\theta}^2 + \dot{\phi}^2\sin^2\theta\right) - F\left(1 - \cos\theta\right) = 0, \tag{25}$$

$$EI\dot{\phi}\sin^2\theta - C\tau\left(1 - \cos\theta\right) = 0. \tag{26}$$

In Love's theory, the azimuth angle θ remains constant along the rod, giving a continuous helix. In Coyne's analysis, there is no such condition. In order to obtain a localized solution, the θ angle must change. Solving the equations for $\dot{\theta}$ and $\dot{\phi}$ gives

$$\dot{\theta} = 2\sqrt{\frac{F}{EI}}\tan\frac{\theta}{2}\sqrt{\cos^2\frac{\theta}{2} - \frac{(C\tau)^2}{4EIF}}, \tag{27}$$

$$\dot{\phi} = \frac{C\tau}{2EI}\cos^{-2}\frac{\theta}{2}. \tag{28}$$

We observe that $\dot{\theta}$ in a function of only θ and can be integrated to obtain

$$\sin\frac{\theta}{2} = \frac{A}{\cosh(Al/\lambda)}, \tag{29}$$

where A is a dimensionless constant ($A^2 = 1 - (C\tau)^2/4EIF$) and λ the characteristic length ($\lambda = \sqrt{EI/F}$). We should emphasize here that $l = 0$ in the middle of the cable. We observe that the right-hand side of equation 29 is symmetrical about $l = 0$. Therefore θ decreases symmetrically to zero as l goes from zero to plus or minus infinity (figure 5 right). Referring back to equations 25 and 7, we see that curvature equals $\kappa^2 = (2F/EI)(1 - \cos\theta) = (4F/EI)\sin^2(\theta/2)$. This means that the plot in figure 5 is also a plot of curvature versus l/λ.

Up to now, nothing has been said about cable end displacement B. Since the cable is symmetric, the end displacement on each side are the same and equal $B/2 = (l - z)_{end}$. We know that the derivative of $(l - z)$ is $(1 - \dot{z}) = 4\sin^2(\theta/2)$. Using equation 29 with relation $\cosh x = (e^x + e^{-x})/2$ and integrating gives the total end displacement

$$B = 4A\lambda - \frac{8A\lambda}{1 + e^{AL/\lambda}}. \tag{30}$$

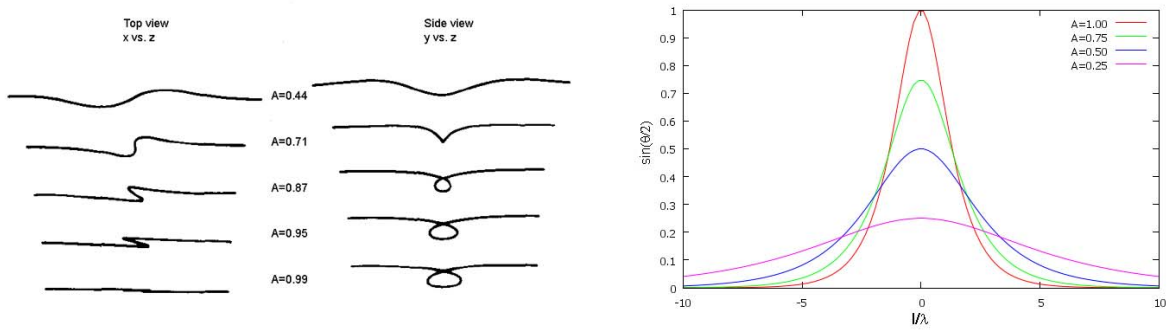

Figure 5: The picture on the right shows some equilibrium configurations of a twisted cable, obtained by numerical integration for different parameters A [3]. The three-dimensional solutions are represented as viewed from the top and from the side. Coordinates are normalized to λ. The graph on the right represents the curvature of a twisted cable versus z/λ for different A. The coefficient A is determined by the boundary conditions for F and τ

The constant of integration $4A\lambda$ is determined by the condition that $l = 0$ when $z = 0$. Observe that $(l - z)$ is otherwise antisymmetric about $l = 0$. The total displacement for a cable whose length is much greater than the dimensions of the loop ($AL/\lambda >> 1$) is $B = 4A\lambda$.

With the cable initially straight with internal twist τ_0, the initial torsional energy E_t per unit length equals $1/2C\tau_0^2$. As the cable ends are allowed to approach one another some of this torsional energy is converted into flexural energy E_f and work done against end forces W. The cable ends are of course restrained from rotating and so there is no torsional work. The energy conservation law states that $dE_t + dE_f + W = 0$.

Letting the cable ends approach one another changes some of the quantities (F, τ, B) that were up to now considered to be constant and determined by the static boundary conditions. Two independent variables specify the boundary condition. In our case, these two variables will be torsion τ and normalized end displacement $B/4\lambda$, with which we may express the energy conservation law.

The work done by the cable on the force F as the cable ends displace is $dW = FdB$. Using the approximate expression $B = 4A\lambda$ and the expressions for A and λ we get

$$dW = \frac{2C\tau d\left(\frac{B}{4\lambda}\right)}{\sqrt{1-\left(\frac{B}{4\lambda}\right)^2}}. \tag{31}$$

Since the torsion is constant along the cable, the change in torsional energy may be expressed by $dE_t = LC\tau d\tau$. The flexural energy per unit length of the cable is $1/2EI\kappa^2$. With equations 25 and 7 we may express the specific flexural energy as $F(1 - \cos\theta)$. But since $F(1 - \cos\theta)dl$ is just $F(dl - dz) = FdB$, we observe that the flexural energy is exactly equal to the work done by the cable on the terminal forces ($dE_f = dW$). This is a consequence of equation 25. Taking these expressions into the energy conservation law yields a new relationship between τ and B

$$d\tau = -\frac{4d\left(\frac{B}{4\lambda}\right)}{L\sqrt{1-\left(\frac{B}{4\lambda}\right)^2}}, \tag{32}$$

which can be integrated to obtain

$$\tau = \tau_0 - \frac{4}{L}\arcsin\left(\frac{B}{4\lambda}\right). \tag{33}$$

Observe that when $B = 4\lambda$, the right-hand side of 44 becomes $\tau_0 - 2\pi/L$. One complete turn is removed from the cable.

The relationship between the terminal force and non-dimensional end displacement is therefore

$$F = \frac{C^2}{4EI}\,\frac{\left(\tau_0 - \frac{4}{L}\arcsin\left(\frac{B}{4\lambda}\right)\right)^2}{\left(1-\left(\frac{B}{4\lambda}\right)^2\right)}. \tag{34}$$

This is not an explicit formula for F because the characteristic length is also a function of force $\lambda = \sqrt{EI/F}$. This formula is the principal solution of Coyne's analysis. It relates the force to the displacement

at the cable ends in terms of the initial twist and cable length. Observe that the force needed to keep the cable straight ($B = 0$) is the same as that of Love's analysis (equation 18). It seems that the two modes of deformation are not succeeding one another but are rather competing with each other.

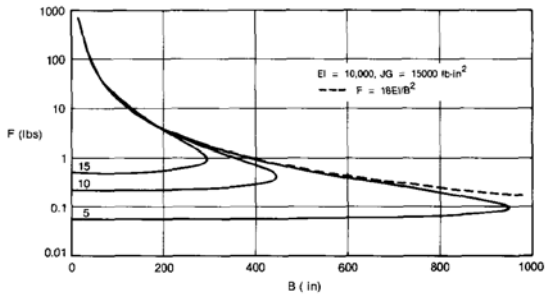

Figure 6: Terminal force F versus total end displacement B for 5, 10 and 15 initial twists [3]. The force at $B = 0$ is given by the criticality condition that has already been obtained by Love. The 'knee' of the curve gives the instability point at which a loop will form.

Figure 6 shows a plot of F versus B for 5, 10 and 15 initial twists. At $B = 0$ the force is given by equation 18. As B increases, approaching the turning point, F and dF/dB increase rapidly. At the turning point dF/dB becomes infinite and B changes direction. The cable has flipped into a loop. The upper branch of the curve represents the tightening of the loop (decreasing B) by applying force after the loop has formed.

The point on the $F(B)$ curve where $dB/dF = 0$ is the called instability point and it represents the point where the cable comes into self-contact. Since B cannot be explicitly expressed, the dB/dF derivative can be obtained with implicit differentiation of equation 34. This gives an equation for cable end displacement B_i at the looping instability point. These calculations are very messy. Fortunately, an approximate solution for long cables exists. It determines the looping instability to be at

$$F_i = \frac{(C\tau_i)^2}{2EI} = \frac{C^2}{2EI}(\tau_0 - \frac{\pi}{L})^2. \tag{35}$$

Notice that this equation is very similar to the criticality condition of Love (equation 18). It is important to understand that this is the point at which the cable comes into self contact. Finding the point at which the loop 'pops out' requires a different approach. The 'pop out' does not occur at the same instability point as the formation of the loop. Our intuition tells us that once the loop has formed increasing the tension will cause the loop to tighten before it pops out.

3.4 Experimental results

Experiments seem to support the theoretical predictions. Thompson and Champneys in [4] performed a number of experiments on metallic wires and rubber rods. The qualitative behavior of both is similar. The rods were loaded onto a testing machine that allowed rigid control of end rotation and end displacement. On some occasions, they were able to observe well developed helices (figure 7 left). On other occasions, there was a fairly continuous transition into the localized deformation of Coyne (figure 8).

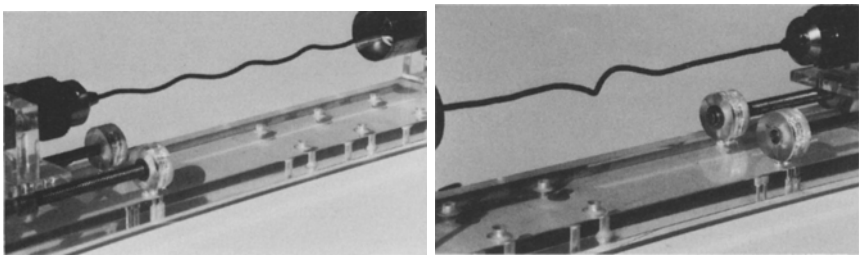

Figure 7: Deformations of a rubber rod due to torsional instability – a continuous helix (left) and a localized deformation of Coyne (right) [4].

Figure 8 shows a tracing of several photographs. A black circular rubber rod was painted half white so that when untwisted it would appear as two parallel black and white strips. The end rotation was

increased in steps of 4π while the end displacements were rigid. Analysis of this figure allows us to distinguish two types of deformation. In the early stages of the twisting process (8π) there is a clearly visible helical deformation H1 which has approximately one full turn per helical wave. This is not the continuous helix that Love predicted. Later in the test (16π) we see that the localized form (L3) has roughly $3 \approx 2(1+\nu)$ turns per wave. This is in agreement with the eigenvalue prediction of Love and also the prediction of Coyne (both arrived at the same criticality condition). Thompson and Champneys predicted that the localized mode L3 would be energetically more favorable one than the H3 that was predicted by Love. And indeed, they were never able to observe the H3 helix in their experiments.

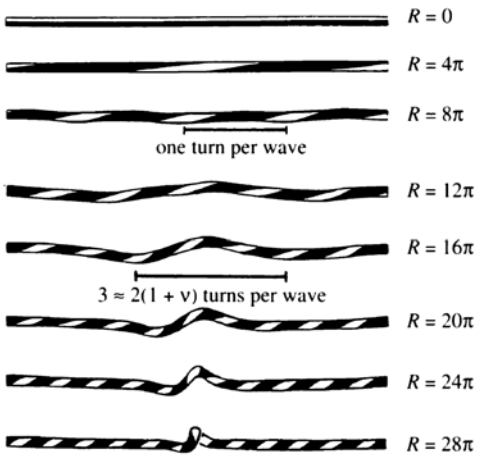

Figure 8: The deformation sequence of one rubber specimen [4]. There is evidence of an initial helical deformation H1. This is followed by a characteristic localization process L3 with approximately three twists per helical wave.

Meanwhile it seems that the short-wave helix H1 either lies outside the domain of Kirchhoff's theory or is associated with the finite length and the boundary conditions. Many approximations were made up to now and so there are many reasons why it might not give a complete description of rubber rods.

4 Formation of plectonemic regions

Twisting an elastic rod will eventually cause it to coil around itself forming a helix (as in figure 3 f). This inter-wound region of the rod is sometimes called the plectonemic region and the straight ends are called the tails. But this newly formed helix is not necessarily uniform. Twisting an elastic cord while keeping the it's ends fixed will result in a non-uniform helix as the one on the left in figure 9. On the other hand, first twisting a cord and then letting the ends approach will result in formation of a non-uniform helix as the one on the right in figure 9. Even though rods are made of very different materials, their qualitative behavior is similar as long as the assumption of linear elasticity holds and there are no plastic deformations.

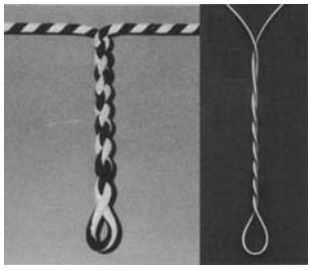

Figure 9: Formation of non-uniform plectonemic regions [4]. The photograph on the right shows a rubber rod that has been continually twisted while its ends were not allowed to approach one another. The photograph on the right shows a cord that has been pre-twisted and then ends were allowed to approach one another.

Any rope maker will tell you that the secret to a uniform tightly laid rope is keeping the plies at

constant tension and letting them gradually coil around one another as we continually twist the seperate plies. This is called compound twisting [12]. Pretwisting separate plies and then twisting them around one another will not produce a tightly laid rope (this is called simple twisting). The reason for this is friction along the contact line of the plies. Friction is also the reason why the non-uniform helices of figure 9 do not redistribute their loops to form a more uniform structure.

Obtaining a nice uniform plectonemic region requires a constant force applied at the rods ends. From now on we will only be interested uniform plectonemic regions. Adding twists will cause the plectonemic region to increase and the tails to shorten. Let l_p represent the length of the rod that makes up the plectonemic region. Then $(L - l_p)$ represents the length of the rod that makes up the tails. A uniform helix is uniquely defined by two parameters. We mentioned before that these two parameters may be the radius R and pitch angle α. The fourth variable, that is significant in this type of twisting, is either the torsion τ or the linking number Lk. The fourth variable tells us how many turns were added into the rod.

We wish to derive the the total energy of this post-buckled state as a function of the four geometrical variables (l_p, α, R and τ). The torsional energy is $C\tau^2 L/2$, since τ is constant along the entire length of the rod. However, the flexural energy is nonzero only in the plectonemic region and therefore equals $EI\kappa^2 l_p/2$. Using equation 11 we see that flexural energy translates to $EIl_p \cos^4\alpha/2R^2$. The potential energy due to external force and torque equals $-F(L - l_p) - 2\pi LkM$, where the linking number is a function of τ, α and R. We have to take into account the fact that the rod is in contact with itself. We replace the actual interaction energy with a constraint term $-\lambda(R - a)$, where λ is the Lagrange multiplier and a the radius of the rod. The total potential energy is given by

$$E(\alpha, R, \tau, l_p) = \frac{1}{2}C\tau^2 L + \frac{1}{2}EI\frac{\cos^4\alpha}{R^2}l_p - F(L - l_p) - M2\pi Lk - \lambda(R - a). \tag{36}$$

The potential energy in itself is not the end result we are interested in. Euler-Lagrange equations give conditions for the mechanical equilibrium of the buckled rod. Differentiating E with respect to the four variables gives four constitutive relations. We will skip these more or less simple calculations for now. We first need to determine which quantities are of interest to us and which are the quantities that can be measured or controlled. We will do this in the next section.

4.1 DNA supercoiling

Deoxyribonucleic acid or DNA is a molecule that is primarily described as a very long double helix. This double helix model describes the local structure of DNA, but the global structure is far more complex. When viewing DNA over long length-scales it may be modeled as a long rod. It is this global structure of DNA that will be the subject of our interest.

In a stress-free configuration of a B-DNA double helix, the two strands twist around the axis once every 10.5 base pairs or every 3.4 nm [13]. The atomic structure of DNA allows for two other possible configurations alternative to the most common B-DNA – A-DNA and Z-DNA. Compared to B-DNA, the A-DNA form is a wider right-handed spiral. In the case of the Z-DNA the strands turn about the helical axis in a left-handed spiral, which is opposite to the more common B form. The radius of a rod-like B-DNA molecule is approximately 1 nm. Adding or subtracting twists to the double helix, as some enzymes can do, imposes strain. The molecule reduces it's twist by coiling around itself as a twisted cable would. The resulting structure is a supercoil.

Extra helical twists are said to be positive and lead to positive supercoiling, while subtractive twisting causes negative supercoiling. DNA of most organisms is negatively supercoiled. Supercoiled DNA forms two structures – a plectonemic or a toroidal (solenoidal) structure, or a combination of both.

This process of supercoiling is of course best described by the linking number. The stress-free configuration of DNA might seem to be twisted. Because of this, White's theorem is sometimes restated as $\Delta Lk = \Delta Tw + Wr$, where ΔTw and ΔLk represent the twists that were added to the initial once-every-10.5-base-pairs twists. For example, a relaxed DNA molecule of monkey virus SV40 with about $5,250$ base pairs has $Lk = Tw \approx 500$ and $\Delta Lk = \Delta Tw = 0$ [13].

Any deformation of DNA involves atomic displacements and should therefore be described at an atomic level. The deformation energy of DNA is governed by base stacking energy, the water–DNA surface interactions, electrostatic interactions along the charged phosphate groups along the DNA [14]. Oftentimes the mechanical properties of DNA can be be described surprisingly well with elastic rod theory. This continuum description of DNA molecules as elastic rods and the corresponding bending and torsional energies have their origin in the nanoscale inter-atomic forces [14].

Studying mechanical properties of DNA became possible with the development of nanotechnology. It is today possible to exert forces onto single DNA molecules. Clauvelin, Audoloy and Neukirch [6] analyze an experiment where one end of the molecule is attached to a glass surface while the other end is attached to a magnetic bead (figure 10). The pulling force and torque are applied with the use of a magnet. The molecule could also have been held by optical tweezers. The linking number of the molecule is increased by rotating the bead while maintaining a constant pulling force (the order of pN). Eventually a plectonemic region forms. The plectonemic phase is not necessarily made up of a single plectonemic structure, but the result is the same as if it were.

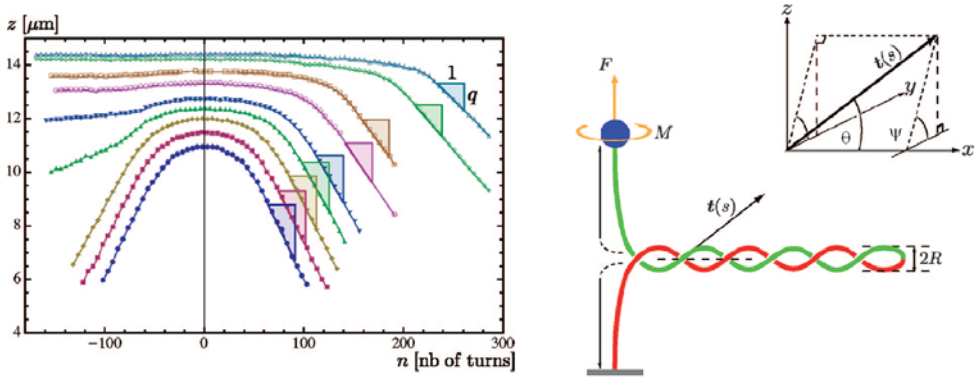

Figure 10: Left: Experimental 'hat' curves showing the vertical extension of the 48 kbp lambda phage DNA molecule as a function of the number of turns imposed on the magnetic bead (salt concentration 10 mM) [6]. Each curve represents a fixed pulling force form 0.25 pN (bottom curve) to 2.95 pN (top curve). The triangles represent the fit for the slope q of the linear region. Right: Schematic representation of the magnetic tweezers experiment [6].

Describing the behavior of DNA with theory of elastic rods is possible only if the radius of the DNA tube-like molecule is not predetermined. The effective radius is defined as the radius of a chargeless, impenetrable elastic tube that has the same mechanical response as the DNA molecule. This radius is not given as a parameter of the model and is extracted from experimental data. The radius varies under changing experimental condition (applied load, salinity, etc.) [6].

In this experiment the controllable quantities are force, number of turns made by the magnetic bead $n = \Delta Lk$ and vertical displacement of the bead $z = L - l_p$. Pitch angle α and helix radius R are the quantities that we are looking for. Euler-Lagrange equations with (36) give two relations that constitute a set of equations for θ and R. Firstly, $\partial E/\partial l_p = 0$ gives the expression [6]

$$F = \frac{EI}{R^2}\sin^4\theta\left(\frac{1}{2} + \frac{1}{\cos 2\theta}\right). \tag{37}$$

The other important relation is the connection between the vertical extension z and the number of turns n imposed on the bead [6]

$$q = \left|\frac{dz}{dn}\right| = \rho_{wlc}\frac{4\pi R}{\sin 2\theta}, \tag{38}$$

where $\rho_{wlc} \in [0, 1]$. The end-to-end distance is shorter than $(L - l_p)$ by a factor of ρ_{wlc}. This factor depends on temperature, bending stiffness, external force and can be determined experimentally through $z(n = 0) = \rho_{wlc}L$. This factor along with the unspecified molecule radius buffer the inter-molecular interactions that actually govern the behavior of DNA.

The graph in figure 10 represents experimental results presented in [6] and [15]. The data is obtained on a 48 kbp (kilo base pair) lambda phage DNA molecule in a 10 mM phosphate buffer. Each curve in the graph corresponds to a given value of the external force (from bottom to top $F = 0.25$, 0.33, 0.44, 0.57, 0.74, 1.10, 1.31, 2.20, 2.95 pN). The linear part of the 'hat' curve represents the region where the plectoneme has already formed. The value of q can be extrapolated from the linear parts of the curve. with this value and the value for F, R and α can be extrapolated with (37) and (38). The calculated values of R and α are graphically represented in figure 11. We see that the radius decreases with increasing force. The pitch angle naturally increases with greater force, as would be expected.

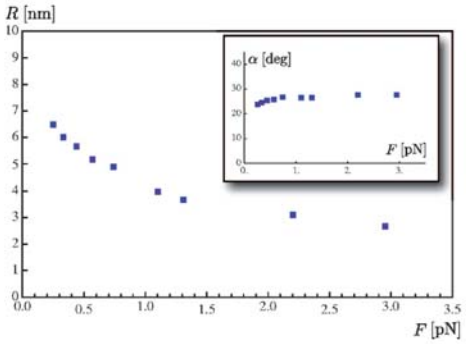

Figure 11: Reconstructions of the plectonemic radius R as a function of the pulling force F. The angle α is shown in the inset [6].

5 Conclusion

There is a relatively continuous transition of the twisted rod from being straight to coiling around itself. We have seen that Coynne's localized L3 solution is energetically more favorable than the continuous helix H3 predicted by Love. However, oftentimes a clearly visible continuous helix H1 can be observed. This helix has approximately one turn per helical wave for a soft rubber rod, whereas Love predicted that it should have 3 turns per helical wave at the bifurcation point. The H1 type of deformation lies outside Kirchhoff's theory. It would seem that there is room for further research in this field of mechanics.

Studying post-buckled states required a new, elegantly simple approach. We simply divided the elastic rod into two regions – the plectonemic region and the tails, disregarding the end loop and the part between the tails and the plectoneme. This enabled us to put down an expression for the total energy of the post-buckled rod. Considering the length of the rod that makes up the plectoneme as a variable gives rise to new analytical solutions for various experimental setups.

In the end we touched on the currently very popular topic – mechanics of DNA molecules. The magnetic tweezers experiment proves to be an indispensable application of the afore mentioned theory.

References

[1] S. Goyal, N. C. Perkins, C. L. Lee, *Torsional buckling and writhing dynamics of elastic cables and DNA*, Proceedings of the ASME 2003 Design Engineering and Technical Conference (2003).

[2] A. E. H. Love, *A treatise on the mathematical theory of elasticity* (Dover Publications, New York, 1927).

[3] J. Coyne, *Analysis of the Formation and Elimination of Loops in Twisted Cable*, IEEE Journal of Oceanic Engineering **15**, 72 (1990).

[4] J. M. T. Thompson, A. R. Champneys, *From helix to localized writhing in the torsional post-buckling of elastic rods*, Proceedings: Mathematical, Physical and Engineering Sciences **452**, 117 (1996).

[5] S. Neukirch, G. H. M. Van der Heijden, *Geometry and mechanics of uniform n-plies*, Journal of Elasticity **69**, 41 (2002).

[6] N. Clauvelin, B. Audoloy, S. Neukirch *Mechanical response of plectonemic DNA: An analytical solution*, Macromolecules **41**, 4479 (2008).

[7] E. H. Dill, *Kirchhoff's theory of rods*, History of Exact Sciences **44**, 1 (1992).

[8] R. Podgornik, *Mehanika kontinuov* (2002).

[9] J. R. Taylor, *Classical mechanics* (University Science Books, 2005).

[10] L. N. Hand, J. D. Finch, *Analytical mechanics* (Cambridge University Press, 1998).

[11] http://www.bioinfo.org.cn/book/biochemistry/chapt23/bio2.htm (17.5.2011).

[12] G. J. Stansfield, *The geometry of twisted multi-filament structures*, British Journal of Applied Physics **9**, 133 (1958).

[13] http://www.bioclassification.org/papers/writhe/2004_Quine.pdf (1 May 2011).

[14] R. Podgornik *Physics of DNA*.

[15] S. Neukirch *Extracting DNA twist rigidity from experimental supercoiling data*, Physical Review Letters **93**, 198107-1 (2004).

[16] http://en.wikipedia.org/wiki/DNA_supercoil (20.4.2011).